AD-A056 837 ANALYTIC SCIENCES CORP READING MASS F/G 8/5
FOURIER PHYSICAL GEODESY.(U)
MAR 78 S K JORDAN F19628-77-C-0152
UNCLASSIFIED TASC-TIM-868-2 AFGL-TR-78-0056 NL

1 OF
AD
A056837

END
DATE
FILMED
9-78
DDC

LEVEL II

12

AFGL-TR-78-0056

FOURIER PHYSICAL GEODESY

Stanley K. Jordan

The Analytic Sciences Corporation
Six Jacob Way
Reading, Massachusetts 01867

1 March 1978

Scientific Report No. 1

Prepared For

AIR FORCE GEOPHYSICS LABORATORY
Air Force Systems Command
United States Air Force
Hanscom Air Force Base, Massachusetts 01731

UNCLASSIFIED

SECURITY CLASSIFICATION OF THIS PAGE (When Data Entered)

(9) Scientific rept. no. 1, 1 May 77-1 Mar 78,

(19) REPORT DOCUMENTATION PAGE

READ INSTRUCTIONS BEFORE COMPLETING FORM

1. REPORT NUMBER (18) AFGL-TR-78-0056	2. GOVT ACCESSION NO. None
3. RECIPIENT'S CATALOG NUMBER	
4. TITLE (and Subtitle) (6) Fourier Physical Geodesy	5. TYPE OF REPORT & PERIOD COVERED Scientific Report No.1 5/1/77 - 3/1/78
(14) TASC	6. PERFORMING ORG. REPORT NUMBER TIM-868-2
7. AUTHOR(s) (10) Stanley K. Jordan	8. CONTRACT OR GRANT NUMBER(s) (15) F19628-77-C-0152 new
9. PERFORMING ORGANIZATION NAME AND ADDRESS The Analytic Sciences Corporation Six Jacob Way Reading, Massachusetts 01867	10. PROGRAM ELEMENT, PROJECT, TASK AREA & WORK UNIT NUMBERS -63701B (16) 7320432AA (17) 32
11. CONTROLLING OFFICE NAME AND ADDRESS Air Force Geophysics Laboratory Hanscom AFB, Massachusetts 01731 Monitor/George Hadgigeorge/LWG	(11) 12. REPORT DATE 1 Mar 78 13. NUMBER OF PAGES 56
14. MONITORING AGENCY NAME & ADDRESS(if different from Controlling Office)	15. SECURITY CLASS. (of this report) UNCLASSIFIED (12) 56p. 15a. DECLASSIFICATION/DOWNGRADING SCHEDULE

16. DISTRIBUTION STATEMENT (of this Report)

Approved for Public Release - Distribution Unlimited

17. DISTRIBUTION STATEMENT (of the abstract entered in Block 20, if different from Report)

18. SUPPLEMENTARY NOTES

19. KEY WORDS (Continue on reverse side if necessary and identify by block number)

Geodesy, Fourier Transform, Gravity

ABSTRACT

20. ABSTRACT (Continue on reverse side if necessary and identify by block number)

Fourier transforms are efficient and convenient for analyzing local gravity data, but the accuracy of Fourier methods is restricted by the flat-earth approximation. In this paper, the theory of matched asymptotic (inner and outer) expansions is used to develop improved flat-earth approximations, determine regions of convergence, and match global (round-earth) and local (flat-earth) gravity models. Accurate solutions in the terms of Fourier transforms are given for the integrals of Poisson, Stokes, and Vening Meinesz. The new theory provides an error analysis of flat-earth algorithms and a systematic procedure for improving their accuracy.

DD FORM 1 JAN 73 1473 EDITION OF 1 NOV 65 IS OBSOLETE

UNCLASSIFIED

SECURITY CLASSIFICATION OF THIS PAGE (When Data Entered)

404 565

TABLE OF CONTENTS

1. INTRODUCTION

The ability of modern instrumentation to collect local gravity data is quickly surpassing our capability to process and interpret this data. For example, the NASA GEOS-3 satellite has already gathered 20 million measurements of geoid height. Storage, analysis, and evaluation of this data is a formidable task.

Fourier transforms are an efficient tool for analyzing such bulk data because space-domain convolutions are replaced by frequency-domain multiplications. In principle, Fourier transforms can be used for almost all data processing tasks: upward continuation, computing anomalies from undulations, smoothing, least-squares collocation, etc. However, Fourier methods are based on the flat-earth approximation. The accuracy of this approximation is therefore a key issue. Flat earth theory is only valid on a local basis, but how large is a "local" area? Do flat-earth methods always lead to long-wavelength errors?

The purpose of this paper is to develop improved flat-earth approximations and thereby enhance the usefulness of Fourier methods in physical geodesy. These improvements are accomplished by treating flat-earth theory as the leading term of an asymptotic expansion.

$$g_{RE} \sim g_{FE} + \varepsilon g_2 + \varepsilon^2 g_3 + \ldots \qquad (1\text{-}1)$$

Here g_{RE} and g_{FE} are round- and flat-earth gravity models. The remaining terms on the right hand side are first- and

higher-order corrections to flat-earth theory. The small parameter ε is inversely proportional to the earth's radius and goes to zero in the limit of large earth radius. As will be shown, the correction terms are relatively easy to calculate using Fourier transforms. Therefore, the flat-earth approximation can be improved to any desired accuracy. In practice, the first correction term is often adequate because the parameter ε is small ($\varepsilon<<1$). Loosely speaking, the parameter ε is small whenever the gravity signals of interest are concentrated in wavelengths that are short relative to the radius of the earth. This situation usually prevails because 90 percent of the energy (variance) in gravity anomalies is contained in wavelengths shorter than 3000 km (Ref. 1).

For typical problems in geodesy, the ("inner") expansion (1) converges only in the vicinity of the point where the flat-earth approximation has been applied. However, this nonuniformity can be corrected by forming an "outer" expansion that is valid at large distances. These expansions are complementary, share an overlapping region of convergence, and can be combined (matched) to produce a uniformly-valid representation of both the local and global field. In this paper, inner and outer expansions are derived and appropriate matching procedures are given.

The approach is based on the theory of matched asymptotic expansions (Refs. 2, 3). This theory was originally developed for boundary-layer problems in fluid mechanics but has found applications in many other areas of applied mathematics. In the present context, flat-earth geodesy is the first term of an inner expansion (Eq. 1-1).

The connection between physical geodesy and boundary-layer theory is not accidental. Gravity anomalies are caused

chiefly by terrain and the associated isostatic compensation at the Mohorovicic discontinuity. Most of the energy in terrain is concentrated in wavelengths that are short relative to earth's radius. Also, the earth's crust is relatively thin compared to the earth's radius. Therefore, a "gravity boundary layer" exists around the earth with a thickness of a few hundred kilometers. Within this boundary layer the flat-earth approximation and Fourier transforms are appropriate. Outside the boundary layer, the curvature of the earth is important and spherical-earth formulas are needed. The theory of matched asymptotic expansions provides a systematic method of matching solutions that are valid inside and outside the boundary layer.

In the next two sections the method of matched expansions is illustrated with examples. These examples provide an introduction to the method but are also important in their own right because they give the appropriate outer expansions that are needed in later sections of the paper.

1.1 DETERMINISTIC EXAMPLE - SHALLOW POINT MASS

The simplest illustration of the flat-earth approximation is a point mass buried at a depth D that is shallow relative to the radius of the earth R_e ($D \ll R_e$). The disturbance potential T is

$$T(r,\psi) = \mu\left[r^2 + (1-\varepsilon)^2 - 2r(1-\varepsilon)\cos\psi\right]^{-1/2} \qquad (1.1\text{-}1)$$

where

$$r = r'/R_e \qquad \varepsilon = D/R_e \qquad (1.1\text{-}2)$$

$$\mu = km/R_e \qquad (1.1\text{-}3)$$

Here r' and ψ are the radius and angle from the center of the earth (Figure 1.1-1). Also, k and m are Newton's gravitational constant and the mass of the disturbing body. The Legendre expansion of Eq. 1.1-1 is

$$T(r,\psi) = \frac{u}{1-\varepsilon} \sum_{n=0}^{\infty} \left(\frac{1-\varepsilon}{r}\right)^{n+1} P_n(\cos\psi) \qquad (1.1\text{-}4)$$

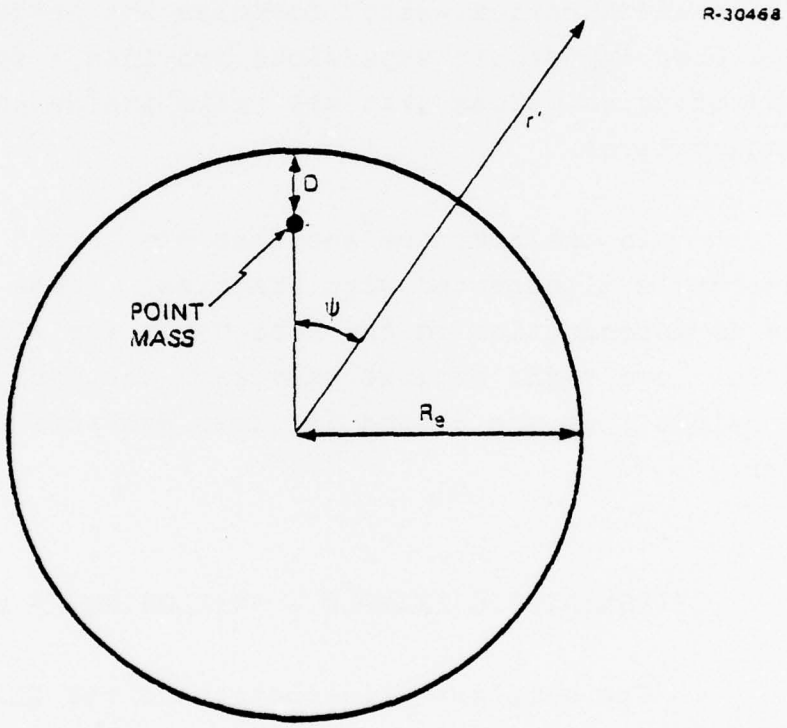

Figure 1.1-1 Notation for Buried Point Mass Example

Because the parameter ε is small, the Legendre series Eq. 1.1-4 converges slowly and is inaccurate for numerical evaluations. A more useful series is obtained by expanding in powers of the parameter ε:

$$T_o(r,\psi) \sim \frac{u}{(r^2+1-2r\cos\psi)^{1/2}} \left[1 + \varepsilon \frac{1-r\cos\psi}{r^2+1-2r\cos\psi} + \ldots\right] \qquad (1.1\text{-}5)$$

However, this series fails to converge in the vicinity of the point mass ($r<1+\varepsilon$ and $\psi<\varepsilon$), as can be seen from the ratio test. In the terminology of perturbation theory, the asymptotic expansion (Eq. 1.1-5) is "nonuniform" and the perturbation problem under consideration is "singular" rather than "regular". Equation 1.1-5 is referred to as an "outer" expansion hence a subscript (T_o) is used.

The standard remedy for such a nonuniform expansion is to define "inner" variables that magnify the region of nonuniformity. This leads to an inner expansion that is valid in the vicinity of the point mass. In general, the appropriate magnification is dictated by the characteristic dimension of the nonuniformity. In this example the altitude (r-1) and angle ψ both need to be stretched by the factor ε. Thus, inner variables (z,R) are defined as

$$z = (r-1)/\varepsilon \qquad \text{and} \qquad R = \psi/\varepsilon \tag{1.1-6}$$

The inner expansion (Eq. 1.1-7) is obtained by substituting Eq. 1.1-6 into Eq. 1.1-1

$$T_i(z,R) \sim \frac{u/\varepsilon}{[(1+z)^2 + R^2]^{1/2}} \left[1 + \frac{\varepsilon}{2} \frac{(1-z)R^2}{(1+z)^2 + R^2} + \ldots\right] \tag{1.1-7}$$

<u>The first term of the inner expansion is the familiar flat-earth approximation</u>. By computing the next term in the series (Eq. 1.1-7) it can be shown that the series diverges for $R>O(1/\sqrt{\varepsilon})$, or equivalently $\psi>O(\sqrt{\varepsilon})$, where O is the usual order symbol. Recall that the outer expansion (Eq. 1.1-5) fails for $\psi<O(\varepsilon)$. Thus, the inner and outer expansions share an overlapping region of convergence $O(\varepsilon) < \psi < O(\sqrt{\varepsilon})$. This overlap implies that a uniformly valid "composite" expansion can be constructed from the inner and outer expansions.

In general a composite expansion can be constructed from an n-term outer expansion and m-term inner expansion, where n and m are positive integers. For simplicity 1-term expansions will be used. First, the common part (cp) of the inner and outer expansions is determined by writing the inner expansion in outer variables and expanding for small ε.

$$cp = \frac{u/\varepsilon}{(z^2 + R^2)^{1/2}} = \frac{u}{[(r-1)^2 + \psi^2]^{1/2}} \qquad (1.1\text{-}8)$$

The same result is obtained by writing the 1-term outer expansion in inner variables and expanding for small ε. Thus, the inner and outer expansions "match" in the overlapping region of convergence. A uniformly valid composite 1-term expansion can be obtained by either the multiplicative or additive rules (Ref. 4).

$$T_c(r,\psi) = T_i T_o / cp \qquad (1.1\text{-}9)$$

$$T_c(r,\psi) = T_i + T_o - cp \qquad (1.1\text{-}10)$$

The additive rule appears more frequently in textbooks (Refs. 2, 3), but the multiplicative rule is more convenient for this example. The multiplicative rule gives

$$T_c(r,\psi) \sim \frac{[(r-1)^2+\psi^2]^{1/2}}{(r^2+1-2r\cos\psi)^{1/2}} \quad \frac{u/\varepsilon}{[(1+z)^2+R^2]^{1/2}} \qquad (1.1\text{-}11)$$

$$= \frac{u}{(r^2+1-2r\cos\psi)^{1/2}} \quad \frac{(z^2 + R^2)^{1/2}}{[(1+z)^2 + R^2]^{1/2}} \qquad (1.1\text{-}12)$$

At low altitudes, the outer expansion and common part cancel each other in Eq. 1.1-11 so that the composite solution is dominated by the inner term. At high altitudes, the inner expansion and common part cancel each other in Eq. 1.1-12 and the outer term dominates.

Errors associated with the various expansions for the potential field of the point mass are illustrated in Figure 1.1-2. The depth of the point mass is 319 km, corresponding to $\varepsilon = 0.05$. The mass of the disturbing body is adjusted so that an undulation of 1 meter is generated directly over the point mass. Figure 1.1-2 shows that the error in the 1-term inner expansion (flat-earth approximation) is zero directly over the point mass (ψ=0), rises to 1 cm at ψ=4 degrees, and rises to 1 cm again at ψ=180 degrees. The 2-term inner expansion is more accurate than the 1-term inner expansion in the vicinity of the point mass (ψ<30 degrees) but suffers the same error growth at large angles. Conversely, the 1-term outer expansion is relatively accurate at large angles (ψ>30 degrees) but inaccurate near the point mass. Thus, the inner and outer expansions are complementary: they provide accuracy in the "near-field" and "far-field", respectively.

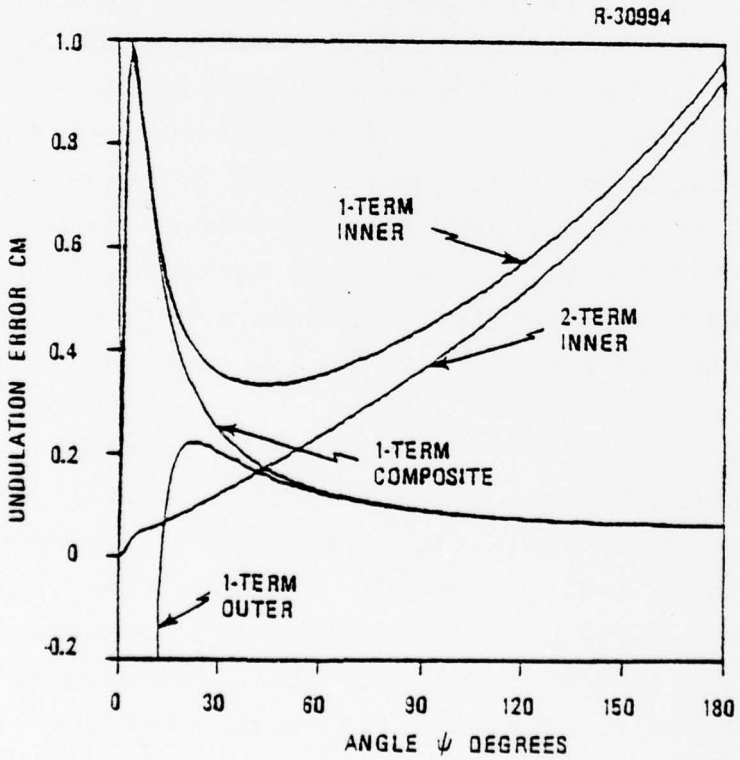

Figure 1.1-2 Errors in Various Expansions of the Undulation Generated by a Shallow Point Mass (ε=0.05, D= 319 km). The Undulation Directly Over the Point Mass is 1 Meter.

A frequency interpretation of the inner and outer expansions can also be made, as follows. The Legendre series corresponding to Eq. 1.1-5 is

$$T_o(r,\psi) = \sum_{n=o}^{\infty} \frac{1}{r^{n+1}} c_n P_n(\cos\psi) \qquad (1.1\text{-}13)$$

$$c_n = (1-\varepsilon)^n \sim \mu(1-n\varepsilon+....) \qquad (1.1\text{-}14)$$

The expansion (Eq. 1.1-14) is accurate for low-order coefficients, but fails for $n>1/\varepsilon$. In other words, the outer expansion (Eq. 1.1-5) provides only long-wavelength information. The inner expansion (Eq. 1.1-7) has the opposite property: it provides only short-wavelength information. Together the two expansions describe the gravity field accurately over all wavelengths.

For comparison, the errors in the various expansions are illustrated in Figure 1.1-3 for a deeper point mass (ε=0.20, D=1270 km). As before, the mass of the disturbing body is adjusted so that an undulation of 1 meter is generated directly over the point mass. The error in the 1-term inner expansion (flat-earth approximation) rises to 4 cm at ψ=18 degrees and again at ψ=180 degrees. The 2-term inner expansion and 1-term outer expansion provide improved accuracy in the near field and far field, as already seen in Figure 1.1-2.

At this point it is worthwhile to review the key ideas. Five formulas have been given for the potential field of a point mass: the exact formula (Eq. 1.1-1) and four expansions - Legendre (Eq. 1.1-4), outer (Eq. 1.1-5), inner (Eq. 1.1-7), and composite (Eq. 1.1-11). The round-earth formulas (Eqs. 1.1-1, 1.1-4 and 1.1-5) are useful at high altitudes ($r>1+\varepsilon$) but inaccurate at low altitudes. (For example, when D=10 km and altitude = 5 km the exact formula and single-precision (7-place) arithmetic yield only 1-place accuracy.) The inner expansion

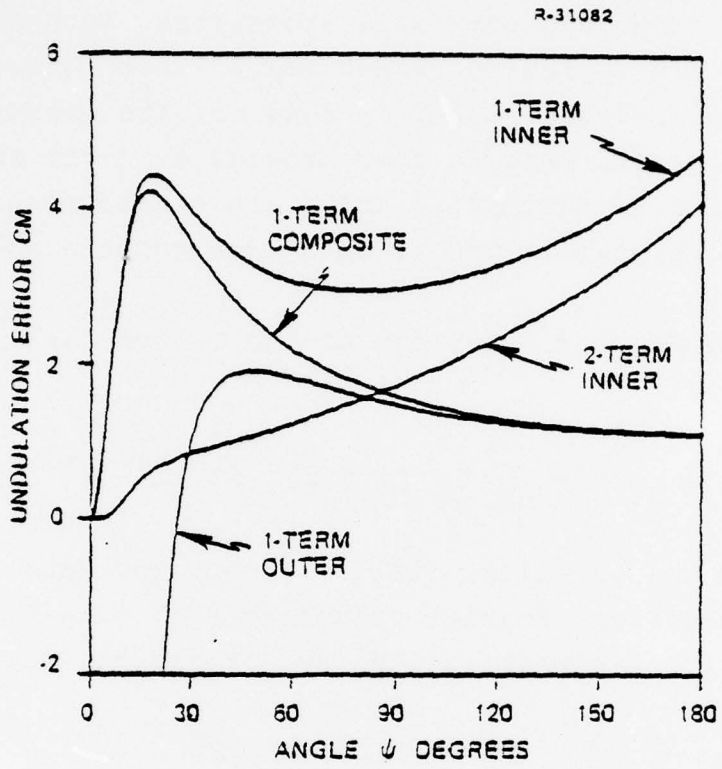

Figure 1.1-3 Errors in Various Expansions for the Undulation Generated by a Shallow Point Mass (ε=0.20, D=1270 km). The undulation Directly Over the Point Mass is 1 Meter.

(Eq. 1.1-7) is useful at low altitudes but fails to converge at large angles ($\psi > 0(\sqrt{\varepsilon})$). The composite expansion (Eq. 1.1-11) enjoys the best properties of round- and flat-earth geodesy: it is accurate everywhere (all altitudes and angles). Generalizing from this example, the following lesson can be drawn. Round- and flat-earth formulas are useful for representing long- and short-wavelength gravity disturbances, respectively. Composite expansions provide a uniformly valid representation over all wavelengths.

It should be emphasized that the usual flat-earth approximation is often adequate. The accuracy improvements

afforded by inner and composite expansions, such as Eqs. 1.1-7 and 1.1-11, are typically rather small (less than one percent in the example, Figure 1.1-2). However, the expansions are still quite useful because they provide an error analysis of the flat-earth approximation and a systematic method for improving the approximation, if such improvements are needed.

The Fourier transform of the 1-term inner expansion is defined as

$$\bar{T}_1(\omega_1, \omega_2, z) = \int_{-\infty}^{\infty}\int T_1(x,y,z)\ e^{i(\omega_1 x + \omega_2 y)}dxdy \qquad (1.1\text{-}15)$$

Inasmuch as the potential field of the point mass is isotropic, the two-dimensional Fourier transform (Eq. 1.1-15) can be written as a one-dimensional Hankel transform (Ref. 5).

$$\bar{T}_1(\omega,z) = 2\pi \int_0^{\infty} RT_1(R,z)\ J_o(\omega R)dR \qquad (1.1\text{-}16)$$

$$= 2\pi(\mu/\varepsilon)\int_0^{\infty} \frac{R}{\left[(1+z)^2 + R^2\right]^{1/2}} J_o(\omega R)dR \qquad (1.1\text{-}17)$$

$$\omega^2 = \omega_1^2 + \omega_2^2 \qquad (1.1\text{-}18)$$

This integral is given by Ref. 6, thus

$$\bar{T}_1(\omega,z) = \frac{2\pi u}{\varepsilon\omega}\ e^{-(1+z)\omega} \qquad (1.1\text{-}19)$$

Notice that the Fourier transform (Eq. 1.1-19) of the point mass field is unbounded at zero frequency.

1.2 STATISTICAL EXAMPLE - ATTENUATED WHITE NOISE ACF

The following model was recently proposed for the gravity disturbance potential autocovariance function (acf) (Ref. 7):

$$\phi(r,\psi) = \frac{\varepsilon^3(2-\varepsilon)^3\,\sigma^2\left[r^2-(1-\varepsilon)^4\right]}{\left[1-(1-\varepsilon)^4\right]\left[r^2+(1-\varepsilon)^4-2(1-\varepsilon)^2\,r\cos\psi\right]^{3/2}} \qquad (1.2\text{-}1)$$

where

$$r = r_1 r_2/R_e^2 \qquad \varepsilon = D/R_e \qquad (1.2\text{-}2)$$

Here r_1, r_2, and ψ are the radii and angular separation of the points being correlated. The model contains two free parameters (σ^2, D) that are fitted to the data. The Legendre expansion of Eq. 1.2-1 is

$$\phi(r,\psi) = \frac{\varepsilon^3(2-\varepsilon)^3\,\sigma^2}{\left[1-(1-\varepsilon)^4\right](1-\varepsilon)^2} \sum_{n=0}^{\infty}(2n+1)\left[\frac{(1-\varepsilon)^2}{r}\right]^{n+1} P_n(\cos\psi) \qquad (1.2\text{-}3)$$

For modeling local (short wavelength) gravity disturbances, the characteristic distance D is small relative to the radius of the earth. (Typically, D=50 km and ε=0.008). Therefore, Eqs. 1.2-1 and 1.2-3 are ill-conditioned and slowly converging, respectively. Expanding in powers of the parameter ε yields

$$\phi(r,\psi) \sim \frac{2\varepsilon^2\,\sigma^2(r^2-1)}{(r^2+1-2r\cos\psi)^{3/2}}\left[1+\varepsilon\,\frac{2(5r^2-1)-2(1+3r^2)r\cos\psi}{(r^2-1)(r^2+1-2r\cos\psi)}\cdots\right] \qquad (1.2\text{-}4)$$

This (outer) expansion diverges when $r<1+0(\varepsilon)$ and $\psi<0(\varepsilon)$. As in the earlier example, inner variables (z,R) are defined by Eq. 1.1-6. The inner expansion is

$$\phi_1(R,z) \sim \frac{4(2+z)\,\sigma^2}{\left[(2+z)^2 + R^2\right]^{3/2}} \left[1+\varepsilon \;\; \frac{z^2(2+z)^2 + 2(3-z^2)\,R^2}{2(2+z)\,[(2+z)^2 + R^2]} + \ldots\right] \tag{1.2-5}$$

As before, the first term of the inner expansion is the familiar flat-earth approximation. The inner expansion fails at high altitudes $(z>2/\varepsilon)$ and large shift distances $\psi>0(1)$.

A composite expansion will now be formed from the 1-term inner and outer expansions. The common part (cp) is

$$cp = \frac{4\sigma^2 z}{(z^2+R^2)^{3/2}} = \frac{4\varepsilon^2\sigma^2(r-1)}{\left[(r-1)^2+\psi^2\right]^{3/2}} \tag{1.2-6}$$

and the multiplicative composite expansion is

$$\phi_c(r,\psi) \sim \frac{\left[(r-1)^2 + \psi^2\right]^{3/2}}{(r^2+1-2r\,\cos\psi)^{3/2}} \;\; \frac{r+1}{2} \;\; \frac{4(2+z)\sigma^2}{\left[(2+z)^2+R^2\right]^{3/2}} \tag{1.2-7}$$

$$= \frac{2\varepsilon^2\sigma^2(r^2-1)}{(r^2+1-2r\,\cos\psi)^{3/2}} \;\; \frac{2+z}{z} \;\; \frac{(z^2+R^2)^{3/2}}{\left[(2+z)^2 + R^2\right]^{3/2}} \tag{1.2-8}$$

The Fourier transform of the 1-term inner expansion is given by Eqs. 1.1-15, 1.1-16 and 1.2-5, thus

$$\phi_1(\omega,z) = 8\pi(2+z)\sigma^2 \int_0^\infty \frac{R}{\left[(2+z)^2 + R^2\right]^{3/2}} \; J_0(\omega R)\,dR \tag{1.2-9}$$

This integral is given in Ref. 6, hence

$$\Phi_1(\omega,z) = 8\pi\sigma^2 \, e^{-(2+z)\omega} \qquad (1.2\text{-}10)$$

Notice that unlike the previous example (Eq. 1.1-19), the Fourier transform (Eq. 1.2-10) is bounded at zero frequency. These transforms (Eqs. 1.1-19 and 1.2-10) are referred to in later sections of the paper.

For simplicity, both the deterministic and statistical examples are based on isotropic gravity fields. For nonisotropic fields, the appropriate transformation between outer variables (r,ψ,α) and inner variables (x,y,z) is

$$x = (\psi/\varepsilon) \sin \alpha \qquad (1.2\text{-}11)$$

$$y = (\psi/\varepsilon) \cos \alpha \qquad (1.2\text{-}12)$$

$$z = (r-1)/\varepsilon \qquad (1.2\text{-}13)$$

The origin of the inner coordinate system is on the surface of the sphere at the center of the local field (e.g., directly above the point mass). The spherical angles ψ and α denote the angular separation and azimuth of a point relative to this origin (Figure 1.2-1).

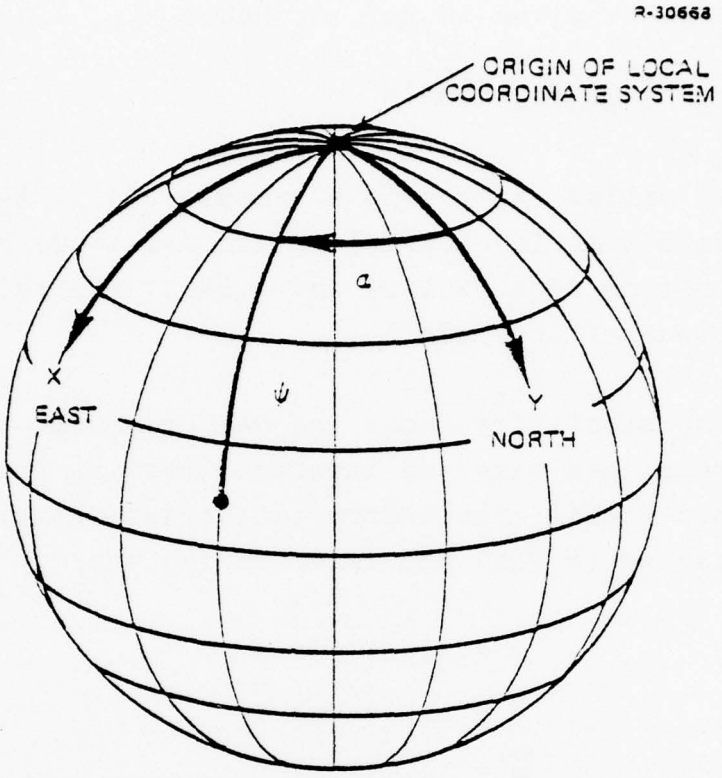

Figure 1.2-1 Definition of Local Coordinates

2. UPWARD CONTINUATION VIA MATCHED ASYMPTOTIC EXPANSIONS

Poisson's integral for upward continuation above a spherical earth is well known (Ref. 8).

$$T(r,\theta,\lambda) = \frac{r^2-1}{4\pi} \int_o^{2\pi} \int_o^{\pi} \ell^{-3}\, T^o(\theta',\lambda')\, \sin\theta'\, d\theta'\, d\lambda' \qquad (2\text{-}1)$$

$$\ell^2 = r^2 + 1 - 2r\cos\psi \qquad (2\text{-}2)$$

$$\cos\psi = \cos\theta\cos\theta' + \sin\theta\sin\theta'\cos(\lambda' - \lambda) \qquad (2\text{-}3)$$

If many evaluations of this integral are needed, it is more efficient to use transforms:

$$T(r,\theta,\lambda) = \sum_{n=o}^{\infty} \frac{1}{r^{n+1}}\, Y_n(\theta,\lambda) \qquad (2\text{-}4)$$

$$Y_n(\theta,\lambda) = \frac{2n+1}{4\pi} \int_o^{2\pi} \int_o^{\pi} T^o(\theta',\lambda')\, P_n(\cos\psi)\, \sin\theta'\, d\theta'\, d\lambda' \qquad (2\text{-}5)$$

However, the harmonic expansion (Eq. 2-4) converges too slowly for modeling local (short-wavelength) gravity disturbances. Local disturbances can be extrapolated aloft with the flat-earth version of Poisson's integral.

$$T(x,y,z) = \frac{z}{2\pi} \iint_{-\infty}^{\infty} \frac{T^o(u,v)\, du\, dv}{\left[(x-u)^2+(y-v)^2+z^2\right]^{3/2}} \qquad (2\text{-}6)$$

Flat-earth upward continuation can also be done using Fourier transforms (Appendix A).

$$T(x,y,z) = \frac{1}{4\pi^2} \iint_{-\infty}^{\infty} \overline{T}^{o}(\omega_1,\omega_2)\, e^{-\omega z}\, e^{-i(\omega_1 x+\omega_2 y)} d\omega_1 d\omega_2 \qquad (2\text{-}7)$$

$$\overline{T}^{o}(\omega_1,\omega_2) = \iint_{-\infty}^{\infty} T^{o}(x,y)\, e^{i(\omega_1 x+\omega_2 y)}\, dxdy \qquad (2\text{-}8)$$

However, the flat-earth formulas (Eqs. 2-6 to 2-8) are only valid in the vicinity of the origin (small x, y and z). Therefore, neither the round- nor flat-earth formulas provide an accurate, uniformly-valid method for upward continuation of local gravity disturbances.

In this section, an inner expansion is derived for upward continuation of local gravity data. The nonuniformity of this expansion at large distances is corrected by matching with an outer expansion. The resulting composite expansion is uniformly valid yet retains the computational advantages of the flat-earth formulas (Eqs. 2-6 to 2-8). In other words, the composite expansion makes it possible to use Fourier transforms for upward continuation and obtain results that are accurate throughout the entire space (r,ϑ,λ) outside the sphere. For simplicity, the derivation is carried out for the special case of an isotropic gravity field. The nonisotropic expansions are inferred.

The disturbance potential satisfies a Dirichlet problem outside a sphere.

$$T_{rr} + \frac{2}{r}\, T_r + \frac{1}{r^2}\, T_{\psi\psi} + \frac{\cot\psi}{r^2}\, T_{\psi} = 0 \quad \begin{cases} 1<r<\infty \\ -\infty<\psi<\infty \end{cases} \qquad (2\text{-}9)$$

$$T = T^{o}(\psi;\varepsilon) \qquad r=1 \tag{2-10}$$

$$T^{o}(\psi;\varepsilon) = T^{o}(\psi+2\pi;\varepsilon) \tag{2-11}$$

Subscripts denote differentiation ($\partial T/\partial r = T_r$). It is assumed that the boundary potential T^o depends on a small parameter ε, and can be expanded in a power series

$$T^{o}(\psi;\varepsilon) \sim T_1^{o}(R) + \varepsilon T_2^{o}(R) + \ldots \quad , \tag{2-12}$$

where $R=\psi/\varepsilon$. An example of such a power series is the shallow point mass, where

$$T^{o}(\psi;\varepsilon) \sim \frac{u/\varepsilon}{(1+R^2)^{1/2}} \left[1 + \frac{\varepsilon}{2} \frac{R^2}{1+R^2} + \ldots\right] \tag{2-13}$$

according to Eq. 1.1-7. In more practical situations such as upward continuation of local gravity data, the dimension of the local field is D, $\varepsilon=D/R_e$, and Eq. 2-12 truncates to a single term ($T_n^o=0$, $n=2,3,\ldots$). (Such an example is given in the next section).

An asymptotic inner expansion is sought of the form

$$T_i(r,\psi;\varepsilon) \sim T_1(z,R) + \varepsilon T_2(z,R) + \ldots \tag{2-14}$$

where $z=(r-1)/\varepsilon$. When Eq. 2-14 is substituted into Eq. 2-9, the following sequence of boundary-value problems is obtained.

First order problem

$$T_{1_{RR}} + \frac{1}{R} T_{1_R} + T_{1_{zz}} = 0 \qquad 0<z<\infty \tag{2-15}$$

$$T_1 = T_1^o(R) \qquad z=0 \tag{2-16}$$

Second-order problem

$$T_{2_{RR}} + \frac{1}{R} T_{2_R} + T_{2_{zz}} = -2z\, T_{1_{zz}} - 2T_{1_z} \tag{2-17}$$

$$T_2 = T_2^o(R) \qquad z=0 \tag{2-18}$$

The solutions are found by Hankel transforms (Ref. 5).

First order solution (isotropic case)

$$T_1(z,R) = \frac{1}{2\pi} \int_0^\infty \omega \overline{T}_1^o(\omega)\, e^{-\omega z}\, J_o(R\omega)\, d\omega \tag{2-19}$$

$$\overline{T}_1^o(\omega) = 2\pi \int_0^\infty R T_1^o(R)\, J_o(R\omega)\, dR \tag{2-20}$$

Second order solution (isotropic case)

$$T_2(z,R) = -\frac{z}{2}(T_1 + z\, T_{1_z}) + \frac{1}{2\pi} \int_0^\infty \omega\, \overline{T}_2^o(\omega)\, e^{-\omega z} J_o(R\omega)\, d\omega \tag{2-21}$$

$$\overline{T}_2^o(\omega) = 2\pi \int_0^\infty R T_2^o(R)\, J_o(R\omega)\, dR \tag{2-22}$$

If the boundary condition is nonisotropic, the Hankel transforms are replaced by Fourier transforms.

First order solution (nonisotropic case)

$$T_1(x,y,z) = \frac{1}{4\pi^2} \int_{-\infty}^{\infty}\int \overline{T}_1^{\circ}(\omega_1,\omega_2)e^{-\omega z}e^{-i(\omega_1 x+\omega_2 y)}d\omega_1 d\omega_2 \tag{2-23}$$

$$\overline{T}_1^{\circ}(\omega_1,\omega_2) = \int_{-\infty}^{\infty}\int T_1^{\circ}(x,y)\, e^{i(\omega_1 x+\omega_2 y)}\, dxdy \tag{2-24}$$

Second order solution (nonisotropic case)

$$T_2(x,y,z) = -\frac{z}{2}\,(T_1 + zT_{1_z}) + \frac{1}{4\pi^2}\int_{-\infty}^{\infty}\int \overline{T}_2^{\circ}(\omega_1,\omega_2)e^{-\omega z}e^{-i(\omega_1 x+\omega_2 y)}\, d\omega_1 d\omega_2 \tag{2-25}$$

$$\overline{T}_2^{\circ}(\omega_1,\omega_2) = \int_{-\infty}^{\infty}\int T_2^{\circ}(x,y)\, e^{i(\omega_1 x+\omega_2 y)}\, dxdy \tag{2-26}$$

A comparison of Eqs. 2-7 and 2-23 reveals that the first term of the inner expansion (Eq. 2-14) is the familiar flat-earth approximation. This confirms that Eqs. 1.2-11 through 1.2-13 is an appropriate choice of inner variables.

The Fourier transform of the two-term inner expansion is

$$\overline{T}_i(\omega_1,\omega_2,z) \sim \overline{T}_1^{\circ}(\omega_1,\omega_2)\, e^{-\omega z}\left[1 - \frac{\varepsilon z}{2}\,(1-\omega z)\right] + \varepsilon\, \overline{T}_2^{\circ}(\omega_1,\omega_2)e^{-\omega z} \tag{2-27}$$

In many cases, such as real data processing, the boundary condition is only one term:

$$T^o(\psi,\alpha;\varepsilon) = T_1^o(x,y) \qquad (2\text{-}28)$$

$$T_n^o(x,y) = 0 \qquad n=2,3,\ldots \qquad (2\text{-}29)$$

This is a special case which simplifies the solutions (Eqs. 2-19 to 2-27). In particular, the parameter ε disappears from the solution, when the solution is written in dimensional form. The dimensional variables are primed:

$$x' = xD \qquad y' = yD \qquad z' = zD \qquad (2\text{-}30)$$

$$\omega_1' = \omega_1/D \qquad \omega_2' = \omega_2/D \qquad \omega' = \sqrt{\omega_1'^2+\omega_2'^2} \qquad (2\text{-}31)$$

The solution (Eq. 2-27) becomes

$$\overline{T}_i(\omega_1',\omega_2',z') \sim \overline{T}^o(\omega_1',\omega_2')e^{-\omega' z'}\left[1 - \frac{z'}{2R_e}(1-\omega' z')\right] \qquad (2\text{-}32)$$

Equation 2-32 provides a very simple recipe for upward continuation of potential field data. First, the data is Fourier transformed to obtain the two-dimensional array $\overline{T}^o(\omega_1,\omega_2)$. This array is multiplied by the appropriate factors in Eq. 2-32 and inverse transformed to obtain the final results. In the limit of large earth radius, Eq. 2-32 degenerates into the usual flat-earth formula. Of course, the inner expansion (Eq. 2-14) is only valid near the origin (small x,y,z). An outer expansion is needed to remove this limitation.

The foregoing analysis provides a method for computing the inner expansion using Hankel or Fourier transforms. Direct integrals can also be used, as shown in Appendix B.

However, the Fourier transforms are more efficient than numerical integration.

The outer expansion will now be constructed. On an outer scale, the local boundary condition Eq. 2-10 shrinks to a point as the parameter ε goes to zero. Therefore, the outer expansion consists of singularity functions that satisfy two requirements: they must obey Laplace's equation and match the inner expansion. Examples of singularity functions that satisfy Laplace's equation have already been studied in the previous sections, namely

$$T(r,\psi) = u(r^2 + 1-2r\cos\psi)^{-1/2} \qquad (2\text{-}33)$$

and

$$T(r,\psi) = \frac{u(r^2-1)}{(r^2+1-2r\cos\psi)^{3/2}} \qquad (2\text{-}34)$$

To match the inner and outer expansions, the 1-term inner expansion is written in outer variables and expanded for small ε.

$$cp = \frac{1}{2\pi}\int_0^\infty \omega\, \overline{T}_1^o(\omega)\, e^{-\omega(r-1)/\varepsilon} J_o(\psi\omega/\varepsilon)\, d\omega \qquad (2\text{-}35)$$

A change of variable ($u=\omega/\varepsilon$) yields

$$cp = \frac{\varepsilon^2}{2\pi}\int_0^\infty u\, \overline{T}_1^o(\varepsilon u)\, e^{-(r-1)u} J_o(\psi u)\, du \qquad (2\text{-}36)$$

The long-wavelength properties of the local field are paramount as ε goes to zero. If the transform $\overline{T}_1^o$ is bounded at zero frequency then Eq. 2-36 becomes

$$cp = \frac{\varepsilon^2}{2\pi}\,\overline{T}_1^o(o)\int_0^\infty u\, e^{-(r-1)u} J_o(\psi u)\, du \qquad (2\text{-}37)$$

$$= \frac{\varepsilon^2}{2\pi} \overline{T}_1^{\circ}(0)\ (r-1)/\left[(r-1)^2 + \psi^2\right]^{3/2} \qquad (2\text{-}38)$$

where

$$\overline{T}_1^{\circ}(0) = 2\pi \int_0^{\infty} R\ T_1^{\circ}(R)\ dR \qquad (2\text{-}39)$$

From the earlier (statistical) example, one can see that Eq. 2-34 is the appropriate singularity for matching Eq. 2-38 with

$$u = \frac{\varepsilon^2}{4\pi}\ \overline{T}_1^{\circ}(0) \qquad (2\text{-}40)$$

The 1-term multiplicative composite expansion is

$$T_c(r,\psi) \sim \frac{\left[(r-1)^2+\psi^2\right]^{3/2}}{(r^2+1-2r\cos\psi)^{3/2}}\ \frac{r+1}{2}\ T_1(z,R) \qquad (2\text{-}41)$$

Here $T_1(z,R)$ denotes the first term of the inner expansion, namely Eq. 2-19.

Returning now to Eq. 2-36, suppose that the transform $\overline{T}_1^{\circ}$ is unbounded at zero frequency as in the first example (Eq. 1.1-19). If the local field satisfies

$$\lim_{\omega \to 0}\ \omega\ \overline{T}_1(\omega) = A \qquad (2\text{-}42)$$

where A is a constant, then Eq. 2-36 becomes

$$cp = \frac{A\varepsilon}{2\pi} \int_0^{\infty} e^{-(r-1)u}\ J_0(\psi u)\ du \qquad (2\text{-}43)$$

$$= \frac{A\varepsilon}{2\pi}\ \left[(r-1)^2+\psi^2\right]^{-1/2} = \frac{A}{2\pi}(z^2+R^2)^{-1/2} \qquad (2\text{-}44)$$

In this case, the appropriate singularity for the outer expansion is Eq. 2-33 with

$$\mu = A\varepsilon/(2\pi) \tag{2-45}$$

The composite expansion is

$$T_c(r,\psi) \sim \frac{[(r-1)^2+\psi^2]^{1/2}}{(r^2+1-2r\cos\psi)^{1/2}} \quad T_1(z,R) \tag{2-46}$$

Inasmuch as the local boundary condition Eq. 2-10 shrinks to a point as the parameter ε goes to zero, the outer expansion and common part are the same for both isotropic and nonisotropic local fields. Therefore, the appropriate composite expansion for nonisotropic local fields is

$$T_c(r,\psi,\alpha) \sim \frac{[(r-1)^2+\psi^2]^{3/2}}{(r^2+1-2r\cos\psi)^{3/2}} \quad \frac{r+1}{2} \quad T_1(x,y,z) \tag{2-47}$$

if the following integral is bounded and non-zero:

$$\iint_{-\infty}^{\infty} T_1^o(x,y)\, dxdy \tag{2-48}$$

However if the integral (Eq. 2-48) is unbounded and

$$\lim_{\omega\to 0} \left[\omega \iint_{-\infty}^{\infty} T_1^o(x,y)\, e^{i(\omega_1 x+\omega_2 y)}\, dxdy\right] = A \tag{2-49}$$

where A is a constant, then the composite expansion is

$$T_c(r,\psi,\alpha) \sim \frac{[(r-1)^2+\psi^2]^{1/2}}{(r^2+1-2r\cos\psi)^{1/2}} \quad T_1(x,y,z) \tag{2-50}$$

The reader should keep in mind that the composite expansions, such as Eq. 2-41, are uniformly valid. Thus, upward continuations of local fields can be done using flat-earth formulas and when the flat-earth results are multiplied by the appropriate factor in Eq. 2-41, they become valid for all altitudes and angles (all r,ψ).

When processing data, the local field will usually have bounded non-zero energy at zero frequency, i.e., Eq. 2-48 is bounded and non-zero. Therefore, Eq. 2-47 is the appropriate composite expansion. A notable exception to this rule is a local field due to one or more point masses. In this case, Eq. 2-48 is unbounded and Eq. 2-50 is the proper expansion.

Both the disturbance potential and the disturbance potential acf satisfy a Dirichlet problem outside a sphere (Ref. 9). Therefore, expansions for upward continuation of acfs can be inferred from the previous results. For upward continuation of the disturbance potential, (r, ψ, α) denote normalized radius ($r=r'/R_e$), angle, and azimuth. For upward continuation of acfs, (ψ,α) denote the angle and azimuth between the points being correlated and

$$r = r_1 r_2 / R_e^2 \qquad (2\text{-}51)$$

where r_1 and r_2 are the radii of the two points.

3. LIMITED DATA EXAMPLE

The earlier examples are instructive because they provide a simple exposition of the key notions:

- For purposes of modeling local gravity disturbances, matched expansions and Fourier transforms are more accurate and efficient than spherical-earth formulas and Legendre transforms.
- The first term of the inner expansion is the familiar flat-earth approximation. Improved accuracy is obtained by computing additional terms.
- The nonuniformity of the inner expansion at large distances is corrected by outer and composite expansions.

Also, the section on upward continuation shows that the inner expansion can be computed with Fourier transforms.

Unfortunately, neither of the earlier examples address the most common type of local gravity field, namely, the gravity field over a limited patch of the earth's surface. A prototype problem is to compute the exterior potential from data within the patch. The boundary condition is

$$T^{o}(\psi,\alpha;\varepsilon) = \begin{cases} t(x,y) & -1 < x,y < 1 \\ 0 & \text{otherwise} \end{cases} \qquad (3\text{-}1)$$

Presumably, data outside this region is continued upward by some other means. For example, data outside the region might be continued upward using spherical-earth (Legendre transform) methods. Alternatively, if the earth's surface is divided into convenient blocks of data, each block can be continued upward

using Fourier methods. Thus, it is sufficient to consider the problem of a single block. To simplify the following example, a circular area is used, and the boundary potential is constant over the area.

$$T^{o}(\psi;\varepsilon) = \begin{cases} t & \psi<\varepsilon \\ 0 & \psi>\varepsilon \end{cases} \tag{3-2}$$

The more realistic case of a square patch and nonuniform potential can be treated by essentially the same methods. In particular, the 1-term inner and composite expansions for the general case are Eqs. 2-23 and 2-47. Inasmuch as the boundary condition is isotropic, the exact solution Eq. 2-1 can be reduced to a single integral (Ref. 9)

$$T(r,\psi) = \frac{(r^2-1)}{\pi} \int_0^{\pi} \frac{T^{o}(\psi;\varepsilon)\ \sin\theta\ E(v)\ d\theta}{(a-b)\ \sqrt{a+b}} \tag{3-3}$$

where

$$a = r^2+1-2r\ \cos\psi\cos\theta \tag{3-4}$$

$$b = 2r\ \sin\psi\sin\theta \tag{3-5}$$

$$E(v) = \int_0^{\pi/2} \sqrt{1-v^2\ \sin^2 x}\ dx \tag{3-6}$$

$$v^2 = 2b/(a+b) \tag{3-7}$$

Here E denotes the complete elliptic integral of the second kind. Substituting Eq. 3-2 into 3-3 yields

$$T(r,\psi) = \frac{(r^2-1)\ t}{\pi} \int_0^{\varepsilon} \frac{\sin\theta\ E(v)\ d\theta}{(a-b)\ \sqrt{a+b}} \tag{3-8}$$

The inner expansion will now be constructed. The boundary condition Eq. 3-2 becomes

$$T_1^o(R) = \begin{cases} t & R<1 \\ o & R>1 \end{cases} \tag{3-9}$$

$$T_n^o(R) = 0 \qquad n=2,3,\ldots \tag{3-10}$$

The first-order inner solution is Eq. 2-19 where

$$\overline{T}_1^o(\omega) = 2\pi t \int_0^1 R\, J_o(\omega R)\, dR \tag{3-11}$$

This integral is given by (Ref. 6):

$$\overline{T}_1^o(\omega) = 2\pi(t/\omega)\, J_1(\omega) \tag{3-12}$$

Therefore, the first-order inner solution is

$$T_1(z,R) = t \int_0^\infty e^{-\omega z}\, J_o(\omega R)\, J_1(\omega)\, d\omega \tag{3-13}$$

This integral cannot be expressed in terms of elementary functions. The second-order inner solution is

$$T_2(z,R) = -\frac{z}{2}\,(T_1 + z\, T_{1_z}) \tag{3-14}$$

Inasmuch as the transform $\overline{T}_1^o$ is bounded at zero frequency, the 1-term outer expansion is Eq. 2-34 with

$$\mu = \frac{\varepsilon^2}{4\pi}\, \overline{T}_1^o(0) = \varepsilon^2 t/4 \tag{3-15}$$

The 1-term composite expansion is Eq. 2-41.

For the special case $\psi=0$, both the exact solution (Eq. 3-8) and matched expansions can be evaluated in terms of elementary functions. The exact solution (Eq. 3-8) becomes

$$T(r,o) = \frac{(r+1)t}{2r} \left[1 - (r-1)/(r^2+1-2\ r\ \cos\varepsilon)^{1/2}\right] \qquad (3\text{-}16)$$

The first-order inner solution can be evaluated from either the Hankel transform Eq. 3-13 or the direct integral Eq. B-1:

$$T_1(z,o) = t\ (1 - z/\sqrt{1+z^2}) \qquad (3\text{-}17)$$

The 1-term outer expansion Eq. 2-34 for $\psi=0$ is

$$T_o\ (r,o) \sim (\varepsilon^2 t/4)\ \frac{r+1}{(r-1)^2} \qquad (3\text{-}18)$$

and the 1-term multiplicative composite expansion is

$$T_c\ (r,0) \sim \frac{r+1}{2}\ t\ \ (1 - z/\sqrt{1+z^2}) \qquad (3\text{-}19)$$

The second-order inner solution is

$$T_2\ (z,0) = -t(z/2) \left[1 - z\ \frac{2+z^2}{(1+z^2)^{3/2}}\right] \qquad (3\text{-}20)$$

Notice that for a local gravity disturbance ($\varepsilon<<1$), the exact solutions (Eqs. 3-8 and 3-16) are numerically ill-conditioned. The spherical-earth formulas do not provide an accurate, efficient method for upward continuation. However, the matched expansion (Eq. 3-19) is accurate, efficient, and uniformly valid. Furthermore, the matched expansion can be easily improved, if necessary, by adding an additional term to the inner and/or outer expansion. If more accuracy is needed in the near field, another term is added to the inner expansion. Similarly, another term in the outer expansion improves accuracy in the far field.

4. STOKES' INTEGRAL VIA MATCHED ASYMPTOTIC EXPANSIONS

Stokes' integral relates gravity anomalies to the disturbance potential on the sphere

$$T(\theta,\lambda) = \frac{R_e}{4\pi} \int_0^{2\pi} \int_0^{\pi} \Delta g(\psi,\alpha)\, S(\psi)\, \sin\psi\, d\psi\, d\alpha \qquad (4\text{-}1)$$

where S is Stokes' function (Ref. 8). If many evaluations of this integral are needed, a spherical harmonic transform is useful.

$$T(\theta,\lambda) = R_e \sum_{n=0}^{\infty} \frac{\Delta g_n}{n-1} \qquad (4\text{-}2)$$

$$\Delta g_n = \frac{2n+1}{4\pi} \int_0^{2\pi} \int_0^{\pi} \Delta g(\theta',\lambda')\, P_n(\cos\psi)\, \sin\theta'\, d\theta'\, d\lambda' \qquad (4\text{-}3)$$

However, the harmonic series (Eq. 4-2) converges too slowly for modeling local (short-wavelength) gravity anomalies. The disturbance potential due to local gravity anomalies can be computed using the flat-earth version of Stokes' integral (Ref. 10).

$$T(x,y) = \frac{D}{2\pi} \int_{-\infty}^{\infty} \int \frac{\Delta g(u,v)\, du\, dv}{[(x-u)^2 + (y-v)^2]^{1/2}} \qquad (4\text{-}4)$$

The flat-earth computation can also be carried out using Fourier transforms (Appendix A).

$$T(x,y) = \frac{D}{4\pi^2} \int_{-\infty}^{\infty} \int (1/\omega)\overline{\Delta g}\,(\omega_1,\omega_2)\, e^{-i(\omega_1 x+\omega_2 y)}\, d\omega_1 d\omega_2 \qquad (4\text{-}5)$$

$$\overline{\Delta g}(\omega_1,\omega_2) = \int_{-\infty}^{\infty} \int \Delta g(x,y)\, e^{\,i(\omega_1 x+\omega_2 y)}\, dxdy \qquad (4\text{-}6)$$

However, the flat-earth formulas (Eqs. 4-4 through 4-6) are only valid in the vicinity of the origin (small x,y). Therefore, neither the round- nor flat-earth formulas provide an accurate, uniformly-valid method for computing the disturbance potential from local gravity anomalies.

In this section, inner, outer, and composite expansions are derived for computing the disturbance potential from local gravity anomalies. As in the previous section, the derivation is carried out for the isotropic case and corresponding non-isotropic results are inferred.

Stokes' integral is the solution to the differential equation

$$rT_r + 2T = -f(r,\psi) \tag{4-7}$$

The function f ($f=r'\Delta g$) satisfies a Dirichlet problem outside the sphere

$$f_{rr} + \frac{2}{r} f_r + \frac{1}{r^2} f_{\psi\psi} + \frac{\cot\psi}{r^2} f_\psi = 0 \tag{4-8}$$

$$f = f^o(\psi;\varepsilon) = R_e \Delta g \qquad r=1 \tag{4-9}$$

$$f^o(\psi;\varepsilon) = f^o(\psi+2\pi;\varepsilon) \tag{4-10}$$

As in a previous section asymptotic expansions are assumed of the form Eq. 2-14 and

$$f(r,\psi;\varepsilon) \sim f_1(z,R) + \varepsilon f_2(z,R) + \ldots \tag{4-11}$$

$$f^o(\psi;\varepsilon) \sim f_1^o(R) + \varepsilon f_2^o(R) + \ldots \tag{4-12}$$

The following sequence of boundary-value problems is obtained.

First-order problem

$$T_{1_z} = -\varepsilon f_1 \tag{4-13}$$

Second-order problem

$$T_{2_z} = -\varepsilon f_2 - zT_{1_z} - 2T_1 \tag{4-14}$$

The solutions are readily found, inasmuch as the Dirichlet problem was treated in a previous section.

First-order solution (isotropic case)

$$T_1(z,R) = \frac{\varepsilon}{2\pi} \int_0^\infty \overline{f}_1^o(\omega)\, e^{-\omega z}\, J_o(\omega R)\, d\omega \tag{4-15}$$

$$\overline{f}_1^o(\omega) = 2\pi \int_0^\infty R\, f_1^o(R)\, J_o(\omega R)\, dR \tag{4-16}$$

Second-order solution (isotropic case)

$$T_2(z,R) = -zT_1 + \frac{\varepsilon}{2\pi} \int_0^\infty (1/\omega)\, \overline{f}_1^o(\omega)\, e^{-\omega z}\, J_o(\omega R)\, d\omega$$

$$+ \frac{\varepsilon}{2\pi} \int_0^\infty \overline{f}_2(\omega)\, e^{-\omega z}\, J_o(\omega R)\, d\omega \tag{4-17}$$

$$\overline{f}_2^o(\omega) = 2\pi \int_0^\infty R\, f_2^o(R)\, J_o(\omega R)\, dR \tag{4-18}$$

At zero altitude ($z = 0$, $r = 1$) we have

$$T_1(R) = \frac{\varepsilon}{2\pi} \int_0^\infty \overline{f}_1^o(\omega)\, J_o(\omega R)\, d\omega \tag{4-19}$$

$$T_2(R) = \frac{\varepsilon}{2\pi} \int_0^\infty (1/\omega)\, \bar{f}_1^o(\omega)\, J_o(\omega R)\, d\omega + \frac{\varepsilon}{2\pi} \int_0^\infty \bar{f}_2^o(\omega)\, J_o(\omega R)\, d\omega \tag{4-20}$$

The corresponding formulas for the nonisotropic case are:

First-order solution (nonisotropic case)

$$T_1(x,y) = \frac{\varepsilon}{4\pi^2} \int_{-\infty}^{\infty}\int (1/\omega)\, \bar{f}_1^o(\omega_1,\omega_2)\, e^{-i(\omega_1 x+\omega_2 y)}\, d\omega_1 d\omega_2 \tag{4-21}$$

$$\bar{f}_1^o(\omega_1,\omega_2) = \int_{-\infty}^{\infty}\int f_1^o(x,y)\, e^{i(\omega_1 x+\omega_2 y)}\, dxdy \tag{4-22}$$

Second-order solution (nonisotropic case)

$$T_2(x,y) = \frac{\varepsilon}{4\pi^2} \int_{-\infty}^{\infty}\int (1/\omega^2)\, \bar{f}_1^o(\omega_1,\omega_2)\, e^{-i(\omega_1 x+\omega_2 y)}\, d\omega_1 d\omega_2$$

$$+ \frac{\varepsilon}{4\pi^2} \int_{-\infty}^{\infty}\int (1/\omega)\, \bar{f}_2^o(\omega_1,\omega_2)\, e^{-i(\omega_1 x+\omega_2 y)}\, d\omega_1 d\omega_2 \tag{4-23}$$

$$\bar{f}_2^o(\omega_1,\omega_2) = \int_{-\infty}^{\infty}\int f_2^o(x,y)\, e^{i(\omega_1 x+\omega_2 y)}\, dxdy \tag{4-24}$$

A comparison of Eqs. 4-5 and 4-21 reveals that the first term of the inner expansion (Eq. 2-14) is the familiar flat-earth approximation. This confirms that Eqs. 1.2-11 through 1.2-13 is an appropriate choice of inner variables.

The outer expansion will now be constructed by a matching procedur. as was done in a previous section. The

1-term inner expansion (Eq. 4-15) is written in outer variables and expanded for small ε.

$$cp = \frac{\varepsilon}{2\pi} \int_0^\infty \bar{f}_1^o(\omega)\, e^{-\omega(r-1)/\varepsilon}\, J_o(\omega\psi/\varepsilon)\, d\omega \qquad (4\text{-}25)$$

A change of variable ($u=\omega/\varepsilon$) yields

$$cp = \frac{\varepsilon^2}{2\pi} \int_0^\infty \bar{f}_1^o(\varepsilon u)\, e^{-(r-1)u}\, J_o(\psi u)\, du \qquad (4\text{-}26)$$

Assuming that the integral

$$\bar{f}_1^o(0) = 2\pi \int_0^\infty R\, f_1^o(R)\, dR \qquad (4\text{-}27)$$

is bounded and non-zero, Eq. 4-26 becomes

$$cp = \frac{\varepsilon^2}{2\pi} \bar{f}_1^o(0) \int_0^\infty e^{-(r-1)u}\, J_o(\psi u)\, du \qquad (4\text{-}28)$$

$$= \frac{\varepsilon^2}{2\pi} \bar{f}_1^o(0) / \left[(r-1)^2 + \psi^2\right]^{1/2} \qquad (4\text{-}29)$$

The implied singularity in the outer expansion is Eq. 2-33 where

$$\mu = \varepsilon^2 \bar{f}_1^o(0)/(2\pi) \qquad (4\text{-}30)$$

The composite expansion is

$$T_c(r,\psi) \sim \frac{\left[(r-1)^2 + \psi^2\right]^{1/2}}{(r^2+1-2r\cos\psi)^{1/2}}\, T_1(z,R) \qquad (4\text{-}31)$$

At zero altitude ($r=1$, $z=0$) we have

$$T_c(\psi) \sim \frac{\psi}{\sqrt{2}(1-\cos\psi)^{1/2}}\, T_1(R) \qquad (4\text{-}32)$$

$$=(\psi/2)\ \csc(\psi/2)\ T_1(R) \tag{4-33}$$

The corresponding nonisotropic result is

$$T_c(\psi,\alpha) = (\psi/2)\ \csc(\psi/2)\ T_1(x,y) \tag{4-34}$$

The term $(\psi/2)\csc(\psi/2)$ in Eq. 4-34 is a correction factor applied to the flat-earth results. This factor is near unity -- for example, when ψ=10 and 60 degrees, the factor is 1.001 and 1.047, respectively. Equations 4-33 and 4-19 constitute a uniformly-valid solution to Stokes' problem. Local gravity anomalies are processed using the flat-earth formulas; when the results are multiplied by the appropriate factor in Eq. 4-33, they become valid for all angles (ψ).

Returning now to Eq. 4-26, suppose that the integral (Eq. 4-27) is zero. Then Eq. 4-26 becomes

$$cp = \varepsilon^3 B \int_0^\infty u\ e^{-(r-1)u}\ J_\sigma(\psi u)\ du \tag{4-35}$$

$$= \frac{\varepsilon^3 B(r-1)}{[(r-1)^2+\psi^2]^{3/2}} \tag{4-36}$$

where

$$B = \lim_{\omega\to 0} \int_0^\infty R^2\ \overline{f_1^o}(R)\ J_1(\omega R)\ dR \tag{4-37}$$

The implied singularity in the outer expansion is Eq. 2-34 with

$$u = (\varepsilon^3/2)\ B \tag{4-38}$$

The composite expansion is

$$T_c(r,\psi) \sim \frac{[(r-1)^2 + \psi^2]^{3/2}}{(r^2+1-2r\cos\psi)^{3/2}} \frac{r+1}{2} T_1(z,R) \qquad (4\text{-}39)$$

At zero altitude (r=1, z=0) we have

$$T_c(\psi) \sim (\psi^3/8) \csc^3(\psi/2) T_1(R) \qquad (4\text{-}40)$$

The corresponding nonisotropic result is

$$T_c(\psi,\alpha) \sim (\psi^3/8) \csc^3(\psi/2) T_1(x,y) \qquad (4\text{-}41)$$

Note that Eqs. 4-34 and 4-41 apply when the integral (Eq. 4-27) is non-zero and zero, respectively.

5. VENING-MEINESZ INTEGRAL VIA MATCHED ASYMPTOTIC EXPANSIONS

The Vening-Meinesz integral relates gravity anomalies to vertical deflections (Ref. 8).

$$\begin{Bmatrix}\xi(\vartheta,\lambda)\\ \eta(\vartheta,\lambda)\end{Bmatrix} = \frac{1}{4\pi G}\int_0^{2\pi}\int_0^{\pi} \Delta g(\psi,\alpha)\begin{Bmatrix}\cos\alpha\\ \sin\alpha\end{Bmatrix}\frac{dS}{d\psi}\sin\psi d\psi d\alpha \quad (5\text{-}1)$$

For dealing with local (short-wavelength) gravity anomalies, the flat-earth version is convenient (Ref. 10).

$$\begin{Bmatrix}\xi(x,y)\\ \eta(x,y)\end{Bmatrix} = \frac{1}{2\pi G}\int_{-\infty}^{\infty}\int \frac{\Delta g(u,v)}{[(x-u)^2+(y-v)^2]^{3/2}}\begin{Bmatrix}y-v\\ x-u\end{Bmatrix}dudv \quad (5\text{-}2)$$

The flat-earth computations can also be carried out with Fourier transforms

$$\begin{Bmatrix}\xi(x,y)\\ \eta(x,y)\end{Bmatrix} = \frac{1}{4\pi^2 G}\int_{-\infty}^{\infty}\int \frac{i}{\omega}\begin{Bmatrix}\omega_2\\ \omega_1\end{Bmatrix}\overline{\Delta g}(\omega_1,\omega_2)\, e^{-i(\omega_1 x+\omega_2 y)}d\omega_1 d\omega_2 \quad (5\text{-}3)$$

where $\overline{\Delta g}$ is given by Eq. 4-6. However, the flat-earth formulas (Eqs. 5-2 and 5-3) are only valid in the vicinity of the origin (small x,y).

Asymptotic expansions that enjoy the best properties of the round- and flat-earth formulas can be derived by differentiation of the results in the previous section. In

particular, the deflections in the x and y directions are given by

$$\delta_x = \frac{1}{GD} \frac{\partial T}{\partial x} \tag{5-4}$$

$$\delta_y = \frac{1}{GD} \frac{\partial T}{\partial y} \tag{5-5}$$

An inner expansion is sought of the form

$$\delta_{x_i}(\psi, \alpha; \varepsilon) \sim \delta_{x_1}(x,y) + \varepsilon \delta_{x_2}(x,y) + \ldots \tag{5-6}$$

and similarly for δ_y. From Eqs. 4-19 and 4-20 we have

$$\delta_{x_1}(x,y) = \frac{-(x/R)\varepsilon}{2\pi GD} \int_0^\infty \omega \, \overline{f}_1^o(\omega) \, J_1(\omega R) \, d\omega \tag{5-7}$$

$$\delta_{x_2}(x,y) = \frac{-x/R\varepsilon}{2\pi GD} \left[\int_0^\infty \overline{f}_1^o(\omega) \, J_1(\omega R) \, d\omega + \int_0^\infty \omega \, \overline{f}_2^o(\omega) \, J_1(\omega R) \, d\omega \right] \tag{5-8}$$

The corresponding formulas for the nonisotropic case are

$$\delta_{x_1}(x,y) = \frac{-i\varepsilon}{4\pi^2 GD} \int_{-\infty}^{\infty} \int (\omega_1/\omega) \, \overline{f}_1^o(\omega_1, \omega_2) \, e^{-i(\omega_1 x + \omega_2 y)} d\omega_1 d\omega_2 \tag{5-9}$$

$$\delta_{x_2}(x,y) = \frac{-i\varepsilon}{4\pi^2 GD} \int_{-\infty}^{\infty} \int (\omega_1/\omega^2) \, \overline{f}_1^o(\omega_1, \omega_2) \, e^{-i(\omega_1 x + \omega_2 y)} d\omega_1 d\omega_2$$

$$- \frac{i\varepsilon}{4\pi^2 GD} \int_{-\infty}^{\infty}\int (\omega_1/\omega)\, \bar{f}_2^{o}(\omega_1,\omega_2)\, e^{-i(\omega_1 x+\omega_2 y)} d\omega_1 d\omega_2$$

(5-10)

The associated formulas for δ_y are obvious.

The outer expansion will now be constructed by the same matching procedure used in the previous sections. The 1-term inner expansion (Eq. 5-7) is written in outer variables and expanded for small ε.

$$cp = \frac{-(x/R)\varepsilon}{2\pi GD} \int_0^{\infty} \omega \bar{f}_1^{o}(\omega)\, e^{-\omega(r-1)/\varepsilon}\, J_1(\omega\psi/\varepsilon)\, d\omega \qquad (5\text{-}11)$$

A change of variable ($u=\omega/\varepsilon$) yields

$$cp = \frac{-(x/R)\varepsilon^3}{2\pi GD} \int_0^{\infty} u \bar{f}_1^{o}(\varepsilon u)\, e^{-(r-1)u}\, J_1(\psi u)\, du \qquad (5\text{-}12)$$

Assuming that Eq. 4-27 is bounded and non-zero,

$$cp = \frac{(x/R)\varepsilon^3}{2\pi GD} \bar{f}_1^{o}(0)\, \frac{\psi}{[(r-1)^2 + \psi^2]^{3/2}} \qquad (5\text{-}13)$$

The implied singularity in the outer expansion is

$$\delta_x(r,\psi) \sim \frac{\mu r \sin\psi}{(r^2+1-2r\cos\psi)^{3/2}} \qquad (5\text{-}14)$$

where

$$\mu = \frac{(x/R)\varepsilon^3}{2\pi GD} \bar{f}_1^{o}(0) \qquad (5\text{-}15)$$

The 1-term multiplicative composite expansion for both the isotropic and nonisotropic cases is

$$\delta_{x_c}(x,y) \sim (\psi^2/8)\ \sin\psi\ \csc^3(\psi/2)\delta_{x_1}(x,y) \tag{5-16}$$

Returning now to Eq. 5-12, suppose that the integral (Eq. 4-27) is zero. Then Eq. 5-12 becomes

$$cp = \frac{-(x/R)\varepsilon^4}{GD}\ B \int_0^\infty u^2 e^{-(r-1)u} J_1(\psi u)\ du \tag{5-17}$$

$$= \frac{(x/R)\varepsilon^4}{GD}\ B\ \frac{3(r-1)\psi}{\left[(r-1)^2 + \psi^2\right]^{5/2}} \tag{5-18}$$

The implied singularity for the outer expansion is

$$\delta_x(r,\psi) \sim \frac{-3ur\sin\psi\ (r^2-1)}{(r^2+1-2r\ \cos\psi)^{5/2}} \tag{5-19}$$

where

$$\mu = \frac{(x/R)\varepsilon^3}{GD}\ B \tag{5-20}$$

The 1-term multiplicative composite expansion for both the isotropic and nonisotropic cases is

$$\delta_{x_c}(x,y) \sim (\psi^4/32)\ \sin\psi\ \csc^5(\psi/2)\ \delta_{x_1}(x,y) \tag{5-21}$$

The foregoing expansions provide the vertical deflection components (δ_x, δ_y) in the local x,y coordinate system.

A transformation is necessary to convert these components into north and east deflections (ξ,η). This transformation depends on the latitude and longitude of the origin of the local coordinates, as well as the position (x,y) of the point where the deflection is sought. Although tedious, such transformations are elementary, and are not presented here.

6. DISCRETE FOURIER TRANSFORMS

The foregoing theory is suitable for analytical models such as the earlier examples. For numerical models, the discrete Fourier transform is more useful. The disturbance potential T and its transform $\overline{T}$ are both treated as discrete and periodic. The Fourier transform (Eq. 2-8) becomes

$$\overline{T}^{o}_{mn} = \sum_{k=-M/2}^{M/2-1} \sum_{\ell=-N/2}^{N/2-1} T^{o}_{k\ell}\, e^{2\pi i(mk/M+n\ell/N)} \tag{6-1}$$

where the integers k,ℓ,m,n are defined by

$$x = k\,\Delta x \qquad y = \ell\,\Delta y \tag{6-2}$$

$$\omega_1 = m\Omega_1 \qquad \omega_2 = n\Omega_2 \tag{6-3}$$

$$\Omega_1 = \frac{2\pi}{M\Delta x} \qquad \Omega_2 = \frac{2\pi}{N\Delta y} \tag{6-4}$$

For simplicity, M and N are assumed to be even integers. The inverse transform for upward continuation (Eq. 2-7) becomes

$$T_{k\ell} = \frac{1}{NM} \sum_{m=-M/2}^{M/2-1} \sum_{n=-N/2}^{N/2-1} \overline{T}^{o}_{mn}\, e^{-\omega z}\, e^{-2\pi i(mk/M + n\ell/N)} \tag{6-5}$$

where

$$\omega^2 = \omega_1^2 + \omega_2^2 = m^2\Omega_1^2 + n^2\Omega_2^2 \tag{6-6}$$

Fast Fourier transform algorithms are normally based on one-sided transforms whereas Eqs. 6-1 and 6-6 are two-sided. The

appropriate one-sided transforms can be obtained by shifting the summation operators, inasmuch as both the potential field $T_{k\ell}$ and transform $\bar{T}_{mn}$ are periodic. The one-sided transforms are

$$\bar{T}^{o}_{mn} = \sum_{k=o}^{M-1} \sum_{\ell=o}^{N-1} T^{o}_{k\ell} \; e^{\,2\pi i(mk/M + n\ell/N)} \tag{6-7}$$

$$T_{k\ell} = \frac{1}{NM} \sum_{m=o}^{M-1} \sum_{n=o}^{N-1} \bar{T}^{o}_{mn} \; e^{\,-\omega z} \; e^{\,-2\pi i(mk/M + n\ell/N)} \tag{6-8}$$

where

$$\omega^2 = p^2\Omega_1^2 + q^2\Omega_2^2 \tag{6-9}$$

$$p = \left|m - M/2\right| - M/2 \tag{6-10}$$

$$q = \left|n - N/2\right| - N/2 \tag{6-11}$$

As an example of upward continuation using discrete Fourier transforms, consider the potential field of a point mass.

$$D = \text{depth of point mass} = 319 \text{ km} \tag{6-12}$$

$$\Delta x = \Delta y = D/2 = 160 \text{ km} \tag{6-13}$$

$$z = 319 \text{ km} \tag{6-14}$$

$$\text{Case 1:} \quad M = N = 32 \tag{6-15}$$

$$\text{Case 2:} \quad M = N = 64 \tag{6-16}$$

As in the earlier example, the mass of the disturbing body is selected so that an undulation of 1 meter is obtained directly

over the point mass. The point mass is located directly below the center of the square grid. In each case, the potential field of the point mass is computed at zero altitude. These gridded values are continued aloft using the discrete Fourier transforms (Eqs. 6-7 and 6-8). The results are compared with the exact flat-earth solution to assess the errors introduced by the discrete transforms. Profiles of the errors are shown in Fig. 6-1. For the smaller grid, the error is 2 to 3 cm, whereas the larger grid reduces the errors to 0.2 to 0.3 cm. The larger grid is obviously a better approximation of the infinite-length transforms (Eqs. 2-7 and 2-8).

Errors introduced by the flat-earth approximation and discrete Fourier transforms can be compared by examining Figs. 1.1-2 and 6-1. Figure 1.1-2 shows that the flat-earth approximation introduces an error of 1 cm. Thus, the error introduced by discrete transforms is larger than the flat-earth error for the smaller grid (M=N=32) and smaller than the flat-earth error for the larger grid (M=N=64). These results are not surprising because the dimensions of the smaller and larger grids are 5100 x 5100 km and 10,200 x 10,200 km, respectively, whereas the earth's mean radius is 6371 km.

It is interesting to compare the frequency content of the errors introduced by the flat-earth approximation and discrete transforms. The flat-earth error (Fig. 1.1-2) is basically bimodal: a short-wavelength spike appears at ψ=4 degrees and a long-wavelength error appears at ψ=180 degrees. The discrete transform error is also bimodal: short- and long-wavelength errors arise from the discrete spacing and finite length of the data. Of course, these short-wavelength errors decay quickly as altitude increases.

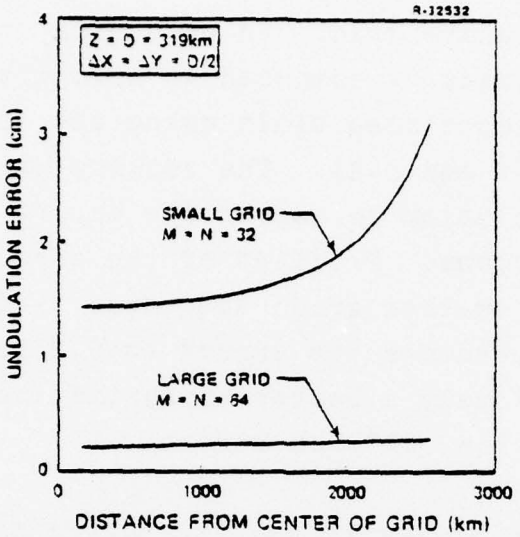

Figure 6-1 Errors in discrete Fourier Transform Upward Continuation of the Undulation Generated by a Shallow Point Mass. The Undulation Directly Over the Point Mass is 1 Meter.

The point mass example is convenient for comparing errors introduced by the flat-earth approximation and finite-length transforms. However, this example is somewhat benign because the potential field tapers smoothly to zero at the edges of the finite grid. Real gravity fields do not taper to zero at the edges and discontinuities appear in a periodic extension. In such cases, the errors introduced by finite-length transforms are more serious than portrayed in the point mass example (Fig. 6-1). However techniques are available for mitigating such "edge effects" (Refs. 11, 14).

For readers who are unfamiliar with the fast Fourier transform, some remarks about computer time are appropriate. The computer time needed for this algorithm tends to be quite minimal, and increases at a relatively modest rate (MN log MN) as the dimension (MxN) of the grid increases (Ref. 12).

The foregoing example problem required 5 seconds of computer time on the IBM 370/158 digital computer, which included four Fourier transforms (two for M=N=32 and two for M=N=64).

7. CONCLUSIONS

Flat-earth formulas provide efficient descriptions of local (short-wavelength) gravity disturbances. The accuracy of this approximation can be improved by the method of matched asymptotic expansions. The inner and outer expansions remove the short- and long-wavelength errors of the flat-earth formulas, respectively. The resulting composite expansions provide uniformly valid descriptions of all wavelengths over all altitudes and distances. The additional computations needed to achieve these accuracy improvements are typically insignificant because the inner expansion is computed using Fourier transforms and the outer expansion consists of simple singularity functions such as Eqs. 2-33 and 2-34.

If discrete rather than continuous Fourier transforms are used, additional errors arise due to the finite spacing and length of the grid. However, these errors can be reduced by using a finer grid spacing, larger grid, and "edge effect" compensation techniques.

APPENDIX A
FOURIER TRANSFORMS OF POISSON AND STOKES' INTEGRALS

The flat-earth Poisson integral (Eq. 2-6) can be viewed as a linear system with the boundary potential T^o and exterior potential T as the input and output. The impulse and frequency response functions are

$$h(x,y) = \frac{z}{2\pi(x^2+y^2+z^2)^{3/2}} \tag{A-1}$$

$$H(\omega_1,\omega_2) = \frac{z}{2\pi}\int_{-\infty}^{\infty}\int (x^2+y^2+z^2)^{-3/2}\, e^{i(\omega_1 x + \omega_2 y)}\, dxdy \tag{A-2}$$

Inasmuch as the impulse response is isotropic, the Fourier transform (Eq. A-2) can be written as a Hankel transform

$$H(\omega_1,\omega_2) = z\int_0^{\infty} R(R^2+z^2)^{-3/2}\, J_o(\omega R)\, dR \tag{A-3}$$

where

$$\omega^2 = \omega_1^2 + \omega_2^2 \tag{A-4}$$

$$R^2 = x^2 + y^2 \tag{A-5}$$

Equation A-3 is the same transform that appears in the statistical example (Eq. 1.2-9) hence

$$H(\omega) = e^{-\omega z} \tag{A-6}$$

which yields Eq. 2-7.

The flat-earth Stokes' integral (Eq. 4-4) can be analyzed similarly. The impulse and frequency response functions are

$$h(x,y) = \frac{D}{2\pi(x^2+y^2)^{1/2}} \tag{A-7}$$

$$H(\omega_1,\omega_2) = \frac{D}{2\pi} \iint_{-\infty}^{\infty} (x^2+y^2)^{-1/2} \, e^{i(\omega_1 x+\omega_2 y)} \, dxdy \tag{A-8}$$

$$= D \int_0^{\infty} J_o(\omega R) \, dR \tag{A-9}$$

This is the same transform that appears in the deterministic example (Eq. 1.1-17) hence

$$H(\omega) = D/\omega \tag{A-10}$$

which yields Eq. 4-5.

APPENDIX B
DIRECT INTEGRAL FORM OF INNER EXPANSIONS

In the text, the inner expansions such as Eq. 2-14 are expressed in terms of Hankel and Fourier transforms, for example, Eqs. 2-19, 2-20 and 2-23, 2-24. These solutions can also be expressed as direct integrals. For example Eqs. 2-19 and 2-20 are replaced by (Ref. 13).

$$T_1(z,R) = \frac{2z}{\pi} \int_0^\infty \frac{T_1^o(u)\ E(\rho)\ udu}{[(R-u)^2+z^2]\,[(R+u)^2+z^2]^{1/2}} \qquad \text{(B-1)}$$

where E is the complete elliptic integral of the second kind (Eq. 3-6) and

$$\rho^2 = \frac{4Ru}{(R+u)^2+z^2} \qquad \text{(B-2)}$$

Equation B-1 effectively replaces two integrals by one. Similarly, the second-order inner solution (Eqs. 2-21 and 2-22) can be expressed as

$$T_2(z,R) = -(z/2)\,(T_1+zT_{1_z}) + \frac{2z}{\pi} \int_0^\infty \frac{T_2^o(u)E(\rho)\ udu}{[(R-u)^2+z^2]\ [(R+u)^2+z^2]^{1/2}} \qquad \text{(B-3)}$$

For the nonisotropic case, Eqs. 2-23 and 2-24 are replaced by

$$T_1(x,y,z) = \frac{z}{2\pi} \int_{-\infty}^{\infty}\int \frac{T_1^o(u,v)\ dudv}{[(x-u)^2+(y-v)^2+z^2]^{3/2}} \qquad \text{(B-4)}$$

Similarly, Eqs. 2-25 and 2-26 are replaced by

$$T_2(x,y,z) = -\ (z/2)\ (T_1+zT_{1_z})$$
$$+ \frac{z}{2\pi} \iint_{-\infty}^{\infty} \frac{T_2^o(u,v)\ dudv}{[(x-y)^2+(y-v)^2+z^2]^{3/2}} \qquad \text{(B-5)}$$

In the Stokes' solution, Eqs. 4-21 through 4-24 are replaced by

$$T_1(x,y) = \frac{\varepsilon}{2\pi} \iint_{-\infty}^{\infty} \frac{f_1^o(u,v)\ dudv}{[(x-u)^2+(y-v)^2]^{1/2}} \qquad \text{(B-6)}$$

and

$$T_2(x,y) = \frac{\varepsilon}{4\pi} \iint_{-\infty}^{\infty} f_1^o(u,v)\ \ln\ [(x-u)^2+(y-v)^2]\ dudv$$
$$+ \frac{\varepsilon}{2\pi} \iint_{-\infty}^{\infty} \frac{f_2^o(u,v)\ dudv}{[(x-u)^2+(y-v)^2]^{1/2}} \qquad \text{(B-7)}$$

In order for the first integral in Eq. B-7 to be bounded, it is required that

$$\iint_{-\infty}^{\infty} f_1^o(x,y)\ dxdy = 0 \qquad \text{(B-8)}$$

The disadvantage of these direct integrals is that numerical integrations are needed for each term of the inner expansion. When Fourier transforms are used, numerical integrations are avoided altogether.

REFERENCES

1. Rapp, R.H., "Geopotential Coefficient Behavior to High Degree and Geoid Information by Wavelength," Dept. Geodetic Science, Ohio State Univ., Report No. 180, Columbus, August 1972.

2. Cole, J.D., Perturbation Methods in Applied Mathematics, Blaisdell Publishing Co., Waltham, Mass., 1968.

3. Nayfeh, A.H., Perturbation Methods, John Wiley and Sons, New York, 1973.

4. Van Dyke, M., Perturbation Methods in Fluid Mechanics, Annotated edition, pp. 94-97, Parabolic Press, Stanford, Calif., 1975.

5. Sneddon, I.N., Fourier Transforms, McGraw-Hill, New York, 1951.

6. Papoulis, A., Systems and Transforms with Application in Optics, p. 145, McGraw-Hill, New York, 1968.

7. Heller, W.G., "A New Self-Consistent Statistical Gravity Field Model," Paper Presented at the Fall Meeting, AGU, San Francisco, Calif., Dec. 1976.

8. Heiskanen, W.A. and Moritz, H., Physical Geodesy, W.H. Freeman, San Francisco, Calif., 1967.

9. Jordan, S.K. and Heller, W.G., "Upward Continuation of Gravity Disturbance Covariance Functions," J. Geophys. Res., to appear.

10. Shaw, L., Paul, I. and Henrikson, P., "Statistical Models for the Vertical Deflection from Gravity Anomaly Models," J. Geophys Res., 74, 4259-4265, 1969.

11. Bhattacharyya, B.K., "Recursion Filters for Digital Processing of Potential Field Data," Geophysics, 41, 712-726, 1976.

12. Brigham, E.O., The Fast Fourier Transform, p. 8, Prentice-Hall, Englewood Cliffs, New Jersey, 1974.

13. Bernstein, U. and Hess, R.I., "The Effects of Vertical Deflections on Aircraft Inertial Navigation Systems," AIAA J., 14, 1377-1381, 1976.

REFERENCES (Continued)

14. Heller, W.G., Tait, K.S. and Thomas, S.W., "GEOFAST — A Fast Gravimetric Estimation Algorithm," The Analytic Sciences Corp., Report No. AFGL-TR-77-0195, August 1977.

Printed by
United States Air Force
Hanscom AFB, Mass. 01731